Foaming of oxidized nanocellulose for the preparation of high-flux water filters

Marta Fortea-Verdejo[1] · Qixiang Jiang[1] · Alexander Bismarck[1,2] · Andreas Mautner[1]

Abstract

Treatment of polluted water is an important task to secure access to clean water also for future generations. Filters are an efficient means to reject various pollutants on a wide range of size scales either by size-exclusion or electrostatic interaction, respectively. Commonly, filters and membranes from various synthetic materials are employed for these applications. Recently, filters based on renewable (nano) cellulose papers and coatings emerged as sustainable alternative to synthetic materials usually utilized. However, fabrication of such paper network structures from aqueous suspension by filtration processes is a time-consuming process caused by the high water holding capacity of highly hydrophilic and negatively charged nanocellulose fibrils. To optimize the preparation of nanocellulose coated filters, substitution of water by air and thus generating nanocellulose foams that are collapsed onto a substrate would be an appealing approach. Here we present the development of foams from negatively charged TEMPO-oxidized nanocellulose by screening various surfactants and concentrations to generate a foam stable enough to be transferred onto a viscose substrate. Foams were collapsed by oven consolidation, positive pressure filtration, or hot-pressing, respectively. Consolidated filters were tested for their water permeance and rejection of heavy metal ions using copper ions as model system. Very high permeances competitive to commercial filters based on synthetic polymers were achieved. Furthermore, adsorption capacities for copper of up to 70 mg/g were found. This is close to adsorption capacities reported for negatively charged TEMPO-oxidized nanocellulose in conventional batch-wise static adsorption. However, in the current process adsorption takes place during filtration of water through filters in a continuous process which constitutes a tremendous advantage.

Graphical Abstract
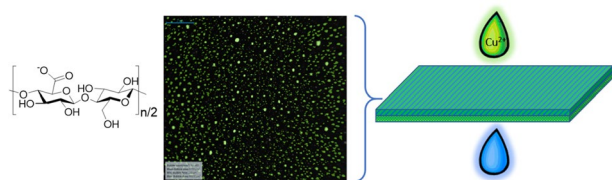
✉ Andreas Mautner
andreas.mautner@univie.ac.at

1 Polymer and Composite Engineering (PaCE) Group, Institute of Materials Chemistry and Research, University of Vienna, Vienna, Austria

2 Department of Chemical Engineering, Imperial College London, London, UK

Introduction

Access to clean water is among the biggest problems human-kind will have to face in the twenty-first century and the water crisis is considered as the number one global societal risk by the WEF. The majority of people living on Earth does not have regular access to clean drinking water and numerous people die each year in connection with polluted water. This all takes place while access to clean drinking

water is one of the most important human rights [1–5]. The problem of water shortage is attributed to over-population, globalization, climate crisis, dietary change, urbanization, and biofuel demand [6]. A further issue is pollution of drinking water resources. It is estimated that > 80% worldwide, and more than 95% in some developing countries, of wastewater is released into the environment without being treated [7]. Thus, launching devices that tackle various kinds of pollutants are urgently required and hence research into new types of materials and approaches for the treatment of both waste and potable water.

Currently, water treatment and devices for treating water are commonly based on synthetic materials, for instance ion-exchange resins or polymer filters and membranes [8–10], or ceramics [11]. These types of materials and devices are frequently highly efficient but regularly add to environmental pollution themselves when disposed of or require vast quantities of energy for their production. To create sustainable water treatment solutions, materials for water treatment devices should originate from renewable sources at low costs. These requirements are very well met by lignocellulosics, i.e., cellulose fibers. A huge variety of conventional natural ligno-cellulosic materials have found applications in the field of water treatment for being available at low cost and potentially even from biomass or industrial side-streams [12]. Unfortunately, often only moderate efficiency of these cheap, renewable materials was achieved at best [13, 14]. Accordingly, more efficient materials sourced from renewable resources should be applied in water treatment. A potential candidate for this purpose could be nanocellulose.

Nanocellulose (NC) is generally composed of cellulose macromolecules that are aligned to form fibrils with diameters between 5 and 100 nm. Due to this small fiber diameter and accordingly high specific surface area (SSA), a high number of hydroxy groups is present on their surface giving rise to electrostatic interactions and also allowing for modification yielding a variety of functional groups. Various classes of NCs are available with strong and flexible cellulose nanofibrils (CNF), fabricated by defibrillation of biomass-fibers using high shear forces, e.g., in mass colliders or high-pressure homogenizers, and cellulose nanocrystals (CNC), obtained by hydrolysis of disordered regions of cellulose fibers with strong acids leaving behind only stiff needle-like crystals, being the most utilized [15].

NCs can be utilized in water treatment in various processes, for instance directly dispersed in suspension as adsorbent ("static batch-wise adsorption") or in the shape of papers or films as filters or membranes [1]. When used as adsorbent, pollutants such as heavy metal ions, dyes,

etc. attach to the surface of the NC fibrils by electrostatic interaction. Successful implementation as adsorbent requires high SSA, as commonly provided by NC, which enables access to functional groups located on the surface [16]. A multitude of pollutants, e.g., heavy metal ions and dyes, can be adsorbed already by natively present hydroxy groups [17], however, by completing various appropriate modification reactions, organic pollutants including dyes, oils, pesticides, and pharmaceuticals are attracted [18, 19], or by attachment of ammonium groups even negatively charged moieties such as nitrates or phosphates can be tackled [20, 21]. Modifying OH-groups to obtain functional groups of higher negative surface charge and thus affinity toward cationic moieties augments adsorption capacities by orders of magnitude. For instance, CNCs prepared by sulfuric or phosphoric acid hydrolysis are inherently equipped with anionic sulfonate or phosphonate groups of high affinity toward dyes and heavy metal ions [18, 22]. Beyond native and inherently present functional groups as well as functional groups introduced during preparation, there is a plethora of options to attach various further functional groups resembling groups frequently utilized in ion-exchange resins [23, 24].

An important compound for water treatment purposes is TEMPO–CNF prepared by (2, 2, 6, 6-tetramethylpiperidine-1-oxyl)-mediated oxidation of cellulose. TEMPO–CNF carry negatively charged carboxylic groups attractive toward cations. TEMPO–CNF were already used for the preparation of nanopaper filters capable of adsorbing heavy metal ions by electrostatic interaction in continuous mode [25, 26]. Pure nanopapers showed reasonable adsorption capacities but exhibited very low permeance due to the dense nature of the random nanofibril network that shapes the nanopapers. To solve this problem, integration of TEMPO–CNF into a network of natural fibers on the microscale, thus forming a hierarchical structure, allowed for high adsorption capacities and very high permeances [26]. However, preparation of such filters requires long fabrication times as filtration of very hydrophilic, water holding TEMPO–CNF is a time-consuming process. Accordingly, circumventing filtration from aqueous dispersion for the production of nanocellulose filters would be key for an efficient process. Replacing water by air by generating a TEMPO–CNF foam and collapsing this foam on a cellulosic microfiber substrate is anticipated to be a very rapid process improving the efficiency of the fabrication process.

Aim of this study was to generate TEMPO–CNF foams capable of being spread on a renewable filter substrate. By investigating different types of surfactants and varying surfactant concentrations, their effect on the bubble dimensions and the foam stability was studied. An optimized

foam precursor was then to be utilized in foam coating studies on a porous viscose substrate to develop water filters with ion capturing performance. Various coating layer grammages and thicknesses, alongside different consolidation methods as well as consolidation temperatures were investigated and permeance as well as ion capture capability evaluated.

Results and discussion

Optimization of the foams

Filters were prepared by application of TEMPO–CNF foamed with either sodium dodecyl sulfate (SDS) or sodium sec-alkyl sulfonate (SAS) on porous viscose substrates. Initially, a foaming process capable of providing sufficiently stable foams for the transfer onto the substrate needed to be established. Albeit TEMPO–CNF are known for stabilization of emulsions [27], their stabilizing effect was not sufficient to obtain foams applicable in a foam coating process. For both types of surfactants, one-tailed anionic SDS and two-tailed anionic SAS, stable foams were obtained at surfactant concentrations > 1.5 wt-%, with respect to the dry weight of TEMPO–CNF. Images of TEMPO–CNF foams

with 1.5 wt-% or 2.4 wt-% of SDS or SAS, respectively, immediately after preparation and after 10 min had elapsed are shown in Figs. 1, 2. Foams prepared with 1.5 wt-% SDS (Fig. 1 top) exhibited a heterogeneous composition of bubbles of various sizes which is indicative of an unstable foam. This is also manifested by the level of the foam being significantly decreased after 10 min (Fig. 1 top right). For SAS (Fig. 1 bottom) on the other hand, a homogeneous arrangement of small bubbles of similar size is present both immediately after preparation and after 10 min had elapsed. This shows that SAS is superior over SDS in terms of stabilization of a liquid foam containing very hydrophilic TEMPO–CNF.

Increasing the surfactant concentration to 2.4 wt-% (Fig. 2 top) yielded a homogeneous foam immediately after preparation also for SDS, however, after 10 min bubbles did coalesce into bigger ones and also the level of the foam height had declined (Fig. 2 top right). For SAS (Fig. 2 bottom), the higher concentration of surfactant resulted in an apparently even more homogeneous foam.

Quantification of these results yielded the number of bubbles per unit area (bubble count) as well as the average area of the bubbles (Fig. 3). As a general rule, the smaller the bubbles and hence their projected area as well as the higher the number of bubbles per area the more stable a foam is

Fig. 1 Photographs taken by the Dynamic Foam Analyser (DFA) of TEMPO–CNF foams prepared with 1.5 wt-% of SDS (top) and SAS (bottom) immediately after preparation (left) and after 10 min had elapsed (right). Magnification = 6×
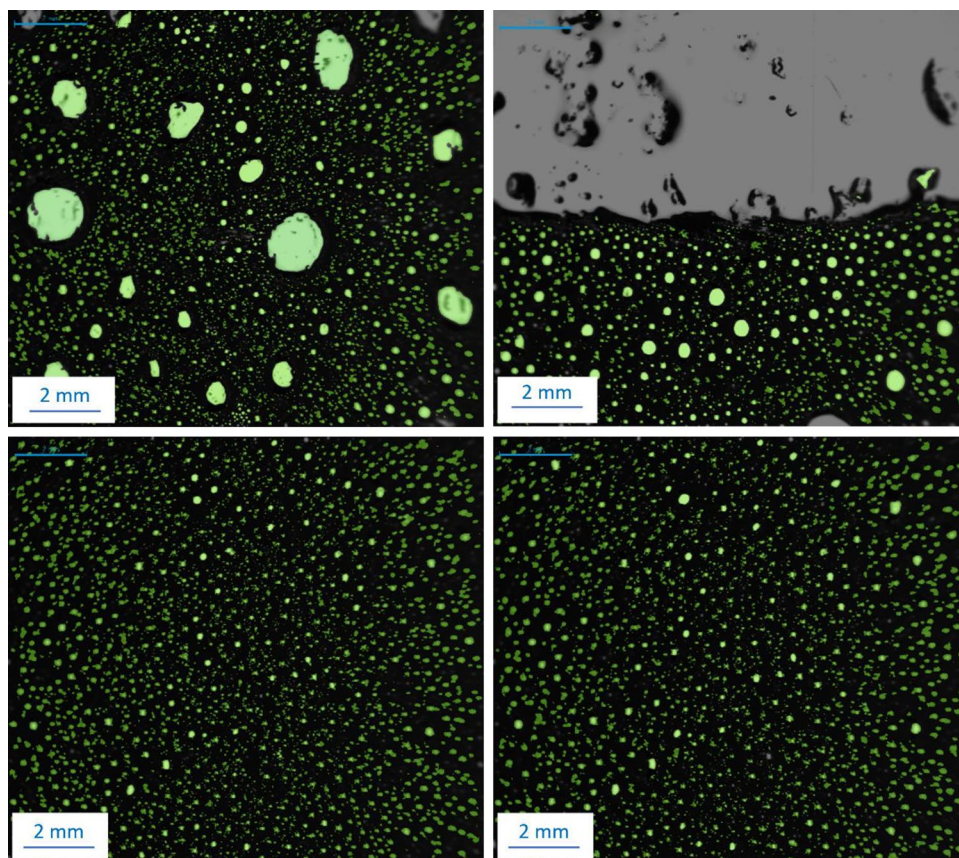
Fig. 2 Photographs taken by the DFA of TEMPO–CNF foams prepared with 2.4 wt-% of SDS (top) and SAS (bottom) immediately after preparation (left) and after 10 min had elapsed (right). Magnification = 6×
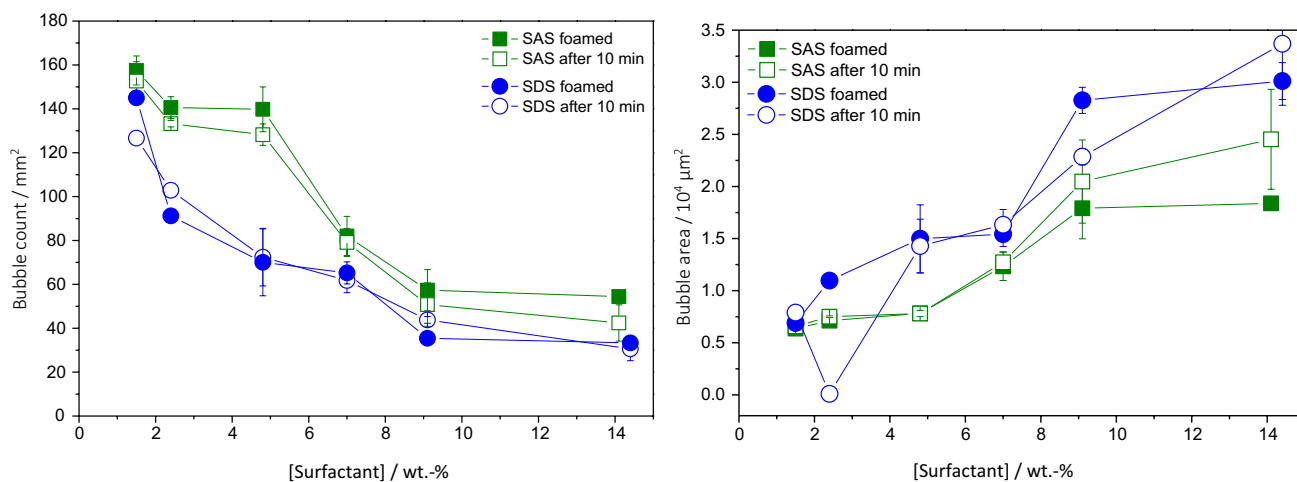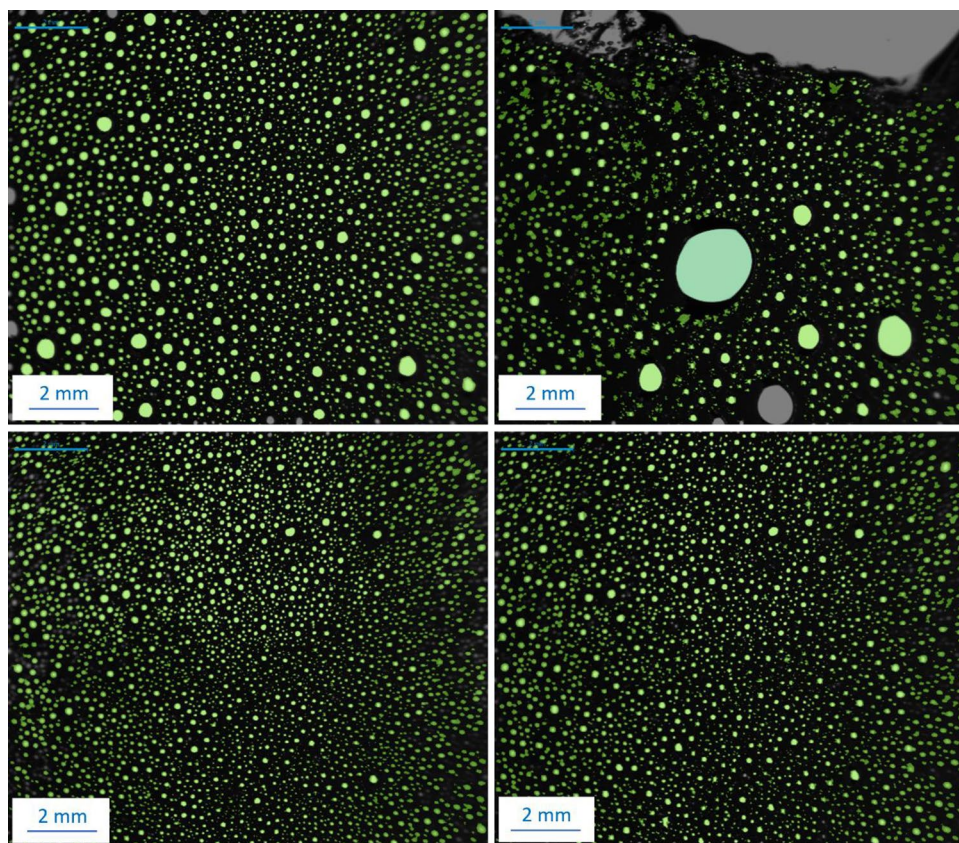

Fig. 3 Results obtained from the DFA: Bubble count (left) and bubble area (right) of TEMPO–CNF foams at different concentrations of SAS (green square) and SDS (blue circle) immediately after foaming (full symbol) and after 10 min had elapsed (open symbol). Error bars indicate the standard deviation of the measurement of several dozens of bubbles (Color figure online)

considered to be. Interestingly, for both types of surfactants the bubble area increased with increasing surfactant concentration while the number of bubbles decreased. Furthermore, at the same surfactant concentration, SAS outperformed SDS in both parameters used to quantify foam stability: higher bubble count and lower bubble area. This was attributed to the two tails of SAS providing better stabilization of the aqueous bubbles around the TEMPO–CNF nanofibrils.
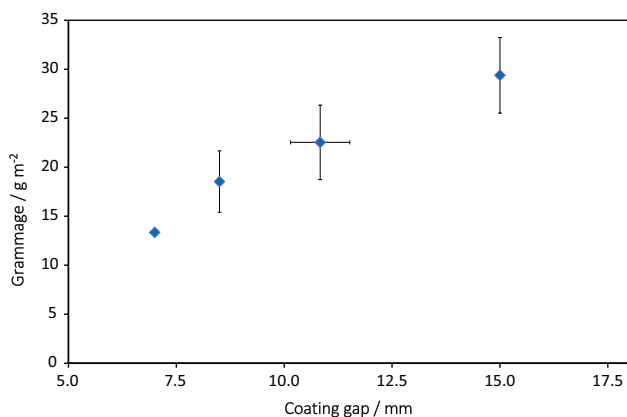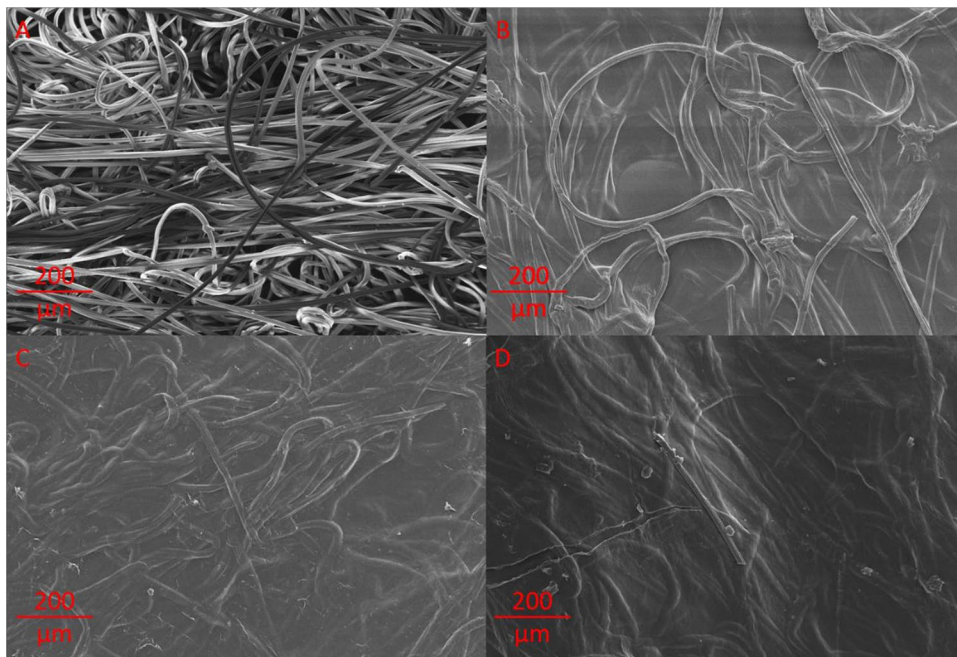
Foam coated filters

Filters were prepared by applying TEMPO–CNF foams on viscose substrates with a roller printer followed by heat-consolidation with three different methods (hot-pressing, positive pressure filtration + oven-drying and oven-drying alone). For all three drying methods for the coated foams prepared with SAS, the grammage of the coating layer in general correlated with the set coater gap (Fig. 4). Variations of the grammage as function of coating gap were attributed to the different drying techniques (oven, positive pressure filtration, and hot-pressing) through which the amount of

foam that was picked up by the filter paper or blotting paper, respectively, during filtration or hot-pressing consolidation varied. Different consolidation temperatures also contributed to this effect. However, there were no general trends identified with regards to the consolidation temperature and therefore data sets grouped to allow for clear identification of the main relationship.

SEM images of foam coated filters consolidated by positive pressure filtration and oven drying in comparison to the virgin viscose substrate are shown in Fig. 5. The thickness of the virgin substrate was about 170 μm, the areal mass ~ 50 g m^{-2}, and the diameters of the viscose fibers were approx. 10 μm. The specific surface area of the substrate was too low to be experimentally determined, e.g., by nitrogen adsorption (BET-model) experiments. From geometrical considerations, taking into account the areal mass and fiber diameter at a fiber density of 1520 kg m^{-3}, the porosity was calculated to be 81%. The geometrical specific surface area thus was ~ 0.08 m^2 g^{-1}, which is more than one order of magnitude below the detection limit of experimental surface area determination.

Filters with various amounts, i.e., coat weights, of foam coated TEMPO–CNF (Fig. 5B–D) all show a similar picture and no apparent differences between filters produced with different consolidation methods could be observed. There was a dense, homogeneous layer of TEMPO–CNF covering the surface of the viscose substrates. Unfortunately, it is not possible to analyze TEMPO–CNF by means of nitrogen adsorption, hence, the overall surface area and porosity of the final filter cannot be determined. The thickness of the layer was apparently increasing with increasing coat

Fig. 5 SEM micrographs of the virgin viscose substrate (A) as well as foam coated, positive-pressure/oven-drying consolidated filters with various coat weights, B: ~ 10 g m^{-2}, C: ~ 20 g m^{-2}, D: ~ 30 g m^{-2}. Magnification = 100×

weights, as can be observed from the micrographs. This was also reflected in an increasing overall thickness of the foam coated filters. However, TEMPO–CNF were not only present on the very surface of the filters but also penetrated into the porous substrate to some extent. Thus, also by geometrical means, it is not possible to determine SSA and porosity and, hence, the structure of the filters can be assessed directly by SEM micrographs but porosity/pore size only indirectly by permeance data.

The thickness of the coating layer was not prone to determination for the nanocellulose partly entered into the porous viscose web during coating. Hence, also the density of the coating and specific surface area available cannot be directly determined and the grammage of the coating is the main parameter to evaluate the filter properties permeance and adsorption capacity. The relationship between permeance and grammage of the coating attached is shown in Fig. 6. Mostly independent of consolidation method and temperature, an inverse logarithmic relationship was found between permeance and grammage. This trend is known for dense stand-alone nanopapers [28–30] but also applies for deposited layers prepared by foam coating. Furthermore, variations of the permeance for filters with similar grammage of the coating were attributed to the different drying procedures and temperatures, however, differences were only minor and no clear relationships could be extracted. Yet, there was a trend observed that filters consolidated by hot-pressing exhibited slightly lower permeances at the same coat weights compared to oven-consolidated filters, which indicated tighter densification of the TEMPO–CNF layer by this process as opposed to oven drying. Overall, permeances of about/more than 100,000 $dm^3\ m^{-2}\ h^{-1}\ MPa^{-1}$ indicate

very low resistance to water passage and are on a level with conventional polymer membranes and higher than most pure nanocellulose membranes [1]. Furthermore, filter's permeance were generally only slighlty below the permeance of the substrate.

Continuous adsorption experiments were performed with model waste water containing copper ions in a concentration similar to highly polluted waste water from industrial effluents [31]. The concentration of various fractions from the filtration experiments were analyzed and the amount of copper adsorbed calculated therefrom plotted vs. the fraction volume. Pure viscose substrates exhibited no detectable adsorption of Cu ions. Exemplarily, the breakthrough curve of dynamic copper adsorption during filtration experiments

Fig. 7 Example for the determination of the adsorption capacity. Areal copper adsorption q_A of a hot-pressed filter with 21.4 gsm as a function of filtration volume. The error bars indicate the standard deviations from three determinations of the concentration and are too small to be observed
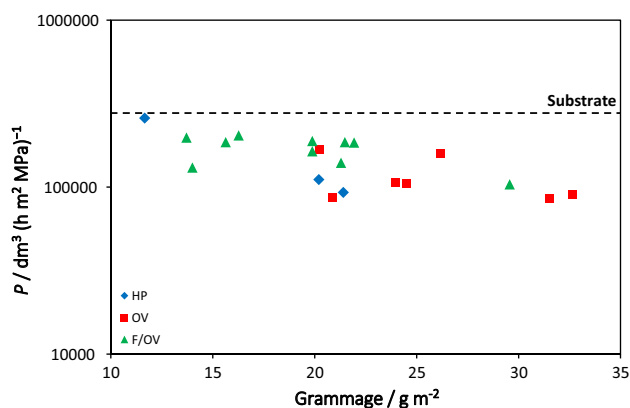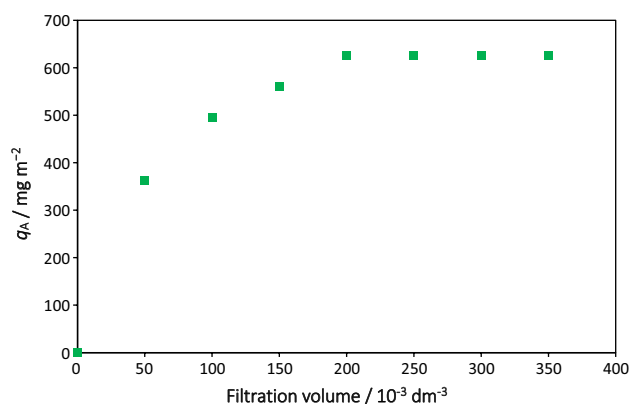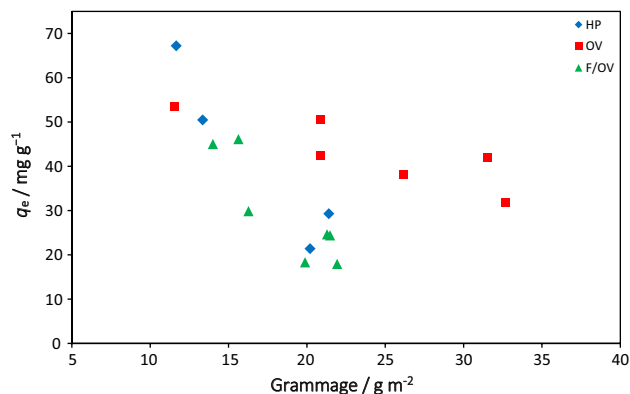
Fig. 6 Pure water permeance of TEMPO–CNF/viscose filters as function of the grammage of the coating layer compared to the virgin substrate (dashed line). Blue diamond: hot-pressed (HP), red square: oven dried (OV), and green triangle: positive pressure filtration/oven dried (F/OV). The measurements were performed until the permeance did not change for more than 2% within one hour, hence, the error bars are too small to be observed (Color figure online)

Fig. 8 Adsorption capacity q_e for copper as a function of the grammage of the coating layer of the filters and their mode of fabrication. Blue diamond: hot-pressed (HP), red square: oven dried (OV), and green triangle: positive pressure filtration/oven dried (F/OV). The error bars indicate the standard deviations from three determinations of the concentration and are too small to be observed

is shown for a hot-pressed filter with 21.4 g per square meter (gsm) coat weight in Fig. 7. The amount of copper adsorbed is apparently very high in the first stages of the filtration with the curve flattening indicating saturation of the filter.

From the total amount of copper adsorbed, the adsorption capacity q_e, i.e., amount of copper per unit mass active adsorption agent (= TEMPO–CNF), was calculated (Fig. 8). Two distinct trends can be read from these data. Filters consolidated by hot pressing and positive pressure filtration exhibited a stronger dependence of the adsorption capacity on the grammage of the coating. Apparently, by hot-pressing and positive pressure filtration denser coatings and hence networks of TEMPO–CNF with smaller pores and lower available surface area were obtained. Unfortunately, it is not possible to determine pore sizes and porosities of TEMPO–CNF structures directly, i.e., by nitrogen adsorption, hence, the trend observed from permeance data that hot-pressing filters results in lower permeance, indicating higher density, confirms this observation. In denser structures, many of the functional carboxylic groups are buried within the "bulk" of the coating and thus not being available for interaction with heavy metal ions on the surface of the filters thus permitting for adsorption. Unfortunately, also the density of a coating on a porous substrate that partly enters into the substrate cannot be directly assessed, however, the trend regarding grammage as function of set coating gap hinted at this phenomenon, too. On the other hand, for oven-only dried filters the correlation between adsorption capacity and grammage of the coating was less pronounced. For these filters, no mechanical consolidation was performed, which is supposed to yield less dense TEMPO–CNF networks providing more available surface area and thus carboxylic groups for adsorption also in the "bulk" of the coating. Anyhow, for all three preparation methods, the highest adsorption capacities were found for the filters exhibiting the lowest grammages of the coating layer. This suggests that also in the case of foam coated porous substrates the majority of adsorption takes place on the very surface of the coating layer and the denser the coating the more distinct this trend. This phenomenon was found before for adsorption of various kinds of ions on pure and dense renewable nanopaper filters [21, 25, 28, 32–35]. Ultimately, adsorption capacities of up to 70 mg g^{-1} were obtained, which is close to the adsorption capacity of TEMPO-CNF in static media but with the benefit of a continuous process [36]. A similar nanocellulose compound, negatively charged phosphorylated nanocellulose exhibits somewhat higher adsorption capacities of about 120 mg g^{-1} [37]. Compared to pure and thus dense nanopapers carrying negatively charged moieties comparable adsorption capacities but much higher permeances were found [32]. In situ modification of nanocellulose paper surfaces obviously yielded much higher adsorption capacities but much lower permeances for the pure and thus denser nanopapers had to be accepted [38]. Compared to porous hierarchical structures composed of natural ligno-cellulosic fibers infused with TEMPO-CNF [26], the same level of adsorption of heavy metal ions was achieved, but preparation of foam coated filters is a much more rapid and thus efficient process than filtration of TEMPO-CNF from aqueous suspension.

Conclusion

We optimized nanocellulose formulations with different types and concentrations of surfactants to prepare TEMPO–CNF foams with appropriate stability for coating on a viscose substrate. We found that two-tailed SAS as surfactant yielded very stable foams suitable for the use in foam coating: more bubbles with lower bubble area and higher stability were obtained compared to using one-tailed SDS as surfactant. Furthermore, no foam decay was observed when SAS was used as surfactant, which was the case with SDS. Moreover, very low surfactant concentrations are sufficient to foam TEMPO–CNF suspensions. TEMPO–CNF foams were coated on a viscose substrate and consolidated by three different drying protocols. Oven drying alone provided the best results in terms of both permeance and adsorption of metal cations on a level with the requirements proposed. Consolidation by hot-pressing or collapsing the foam with positive pressure filtration apparently yielded denser nanocellulose network structures which resulted in lower permeance and adsorption capacity, respectively, due to supposedly smaller pores as well as less available surface area and hence available functional groups. Overall, high adsorption capacities could be paired with very high water permeance, thus indicating highly efficient filtration performance for the continuous adsorption of heavy metal ions. Facilitating attachment of thin negatively charged NC layers on porous cellulosic substrates by deposition of foams constitutes a highly efficient process and generating foam prior to nanocellulose deposition is a process that is relevant on industrial scale and can thus be principally implemented also on larger scale. However, the deposition process needs careful control to obtain optimum layer thickness and appropriate entering and anchoring of the nanocellulose into/on the substrate. Moreover, the production process for TEMPO–CNF still needs to be established at relevant scale and is currently only available at best in pilot scale. Availability of TEMPO–CNF in appropriate quantity and quality at competitive cost is clearly a prerequisite to transfer the process to larger, industrial scale thus permitting for exploitation water treatment properties of NC on relevant magnitude.

Scheme 1
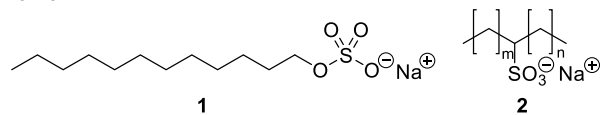
Experimental

TEMPO-oxidized cellulose nanofibrils (TEMPO–CNF) with a charge content of 1.1 mmol g^{-1} were provided by EMPA. Surfactant (Scheme 1) sodium dodecyl sulfate (SDS, **1**) was purchased from Sigma Aldrich and surfactant Hostapur SAS 30 (sodium C14/17 s alkyl sulfonate, SAS, **2**) was kindly supplied by JSP International Sarl. The viscose non-woven web substrate provided by Acondaqua had a thickness of about 170 μm, an areal mass of ~ 50 g m^{-2}, and the diameters of the viscose fibers were approx. 10 μm. Ethylenediaminetetraacetic acid disodium salt dihydrate (EDTA) was purchased from W. Neuber's Enkel and Murexide, ammonia solution, NaOH, copper chloride, and ammonium chloride from Sigma Aldrich. All chemicals were used as received without further purification and ultra-pure water (0.05 μS cm^{-1}, Elga Pure lab) was used for all procedures.

Foam preparation and characterization

Foams were generated by frothing air into nanocellulose suspensions after adding the surfactant directly to 0.06 dm^3 of 0.9 wt-% TEMPO–CNF suspensions. The mixtures (Table 1) were frothed for 90 s at maximum speed (Braun Multimix 5).

Prepared foams were characterized with a Dynamic Foam Analyser (DFA, Krüss). Frothed foams were transferred into the observation tube of the DFA immediately after preparation and the observation started. The amount of bubbles per unit area as well as the area of single bubbles were the main

results of these measurements. For grading the foams, those two parameters were evaluated immediately after preparation and after 10 min had elapsed. A shelf life of the foams of 10 min was considered sufficient to transfer the foam and apply on the substrate before consolidation.

Preparation of foam coated filters

The foams were applied on the viscose substrate by a roller coater (K Printing Proofer) at various coating gaps (Table 2). The value of the set coater gap refers to the gap between the coater and the substrates, it thus defined the thickness of applied foam layers. However, the thickness of the final, consolidated TEMPO–CNF layer was not measurable as part of the TEMPO–CNF penetrated into the substrates rather than merely forming a coating layer on top of the substrates. Consolidation of the foams was performed by three different processes: (i) direct drying in a conventional drying oven at 80, 100, or 120 °C for 30 min, (ii) collapse of the foams in a custom-made positive pressure device at 5 bar for 15 min, followed by consolidation in a drying oven at 80, 100, or 120 °C for 30 min, and (iii) consolidation in a hot-press (Carver) after foam collapse by positive pressure filtration at 120 °C under a mass of 1000 kg for 15 min in a sandwich of blotting papers.

Characterization of the filters

The filters were analyzed regarding their pure water permeance and adsorption capacity for heavy metal ions. Circles of 49 mm diameter were cut from the coated samples and applied on the porous stainless steel support of a dead-end cell (Sterlitech HP 4750). From these specimens also the coat weight was determined by weighing the coated filters

Table 1 TEMPO–CNF-surfactant formulations for foam preparation

Surfactant	TEMPO–CNF/wt-%	Surfactant / wt-% of dry NC
SDS		0.2
		1.5
	0.9	2.4
		4.8
		7.0
SAS		0.2
		1.5
	0.9	2.4
		4.8
		7.0

Table 2 Preparation conditions and parameters for SAS foam coated filters

Method	Set coater gap/mm	Temperature/°C
Oven	8.5	100
	9.5	100
	10.0	100
	10.5	80, 100, 120
	15.0	80, 100, 120
Filtration + oven	8.5	80, 100, 120
	10.5	80, 100, 120
	12.0	80, 100, 120
Hot-press	7.0	120
	9.0	120
	10.5	120
	12.0	120

with known area and relating this to the areal weight of the viscose substrate.

The pure water permeance was determined by forcing (nitrogen head pressure 0.5 bar) deionized water at 20 °C through the coated viscose fabrics (active filtration area of 1460 mm^2). The pure water permeance P (dm^3 m^{-2} h^{-1} MPa^{-1}) was calculated from the measured volume that permeated the filter per unit area per unit time.

For determination of the metal ion adsorption performance, solutions of CuCl$_2$ (10 mmol dm^{-3}) were filtered. Permeate fractions were collected and their concentrations analyzed by colorimetric titration with EDTA against Murexide. The difference of copper concentrations of permeate fractions and the starting solution (c (Cu^{2+})) was calculated and with the fraction volume (V_{fract}) the amount of copper adsorbed per unit area ($A = 1460$ mm^2) or areal adsorption q_A [mg m^{-2}] (Eq. (1)) calculated. q_A was plotted as function of the filtration volume and from the maximum $q_{A,max}$, the adsorption capacity q_e [mg g^{-1}] (Eq. (2)), i.e., the mass of Cu adsorbed per unit mass of the active adsorption agent (G(TEMPO–CNF) [g m^{-2}]), calculated.

$$q_A = \frac{c(\text{Cu}^{2+})}{A \bullet V_{fract}} [\text{mg m}^{-2}] \tag{1}$$

$$q_e = \frac{q_{A,max}}{G(\text{TEMPO} - \text{CNF})} [\text{mg g}^{-1}] \tag{2}$$

Data availability The authors confirm that the data supporting the findings of this study are available within the article.

References

1. Mautner A (2020) Polym Int 69:741
2. Ahuja S (2015) Chemistry and water: the science behind sustaining the world's most crucial resource. Elsevier, Amsterdam, Oxford, Cambridge (MA)
3. WHO (2022) https://www.who.int/news-room/fact-sheets/detail/drinking-water; Accessed 25.07.2022
4. UN general assembly (2010) https://www.un.org/waterforlifedecade/human_right_to_water.shtml; accessed 25.07.2022
5. UNESCO World water assessment programme (2020) https://unesdoc.unesco.org/ark:/48223/pf0000372985.locale=en, Accessed 25.07.2022
6. Chartress C, Varma S (2010) Out of water: from abundance to scarcity and how to solve the world's water problems. FT Press, Upper Saddle River, New Jersey
7. United nations world water assessment programme (2017) http://unesdoc.unesco.org/images/0024/002471/247153e.pdf, Accessed 25.07.2022
8. Paul M, Jons SD (2016) Polymer 103:417
9. Mohammad AW, Teow YH, Ang WL, Chung YT, Oatley-Radcliffe DL, Hilal N (2015) Desalination 356:226
10. Yang Z, Zhou Y, Feng Z, Rui X, Zhang T, Zhang Z (2019) Polymers 11:1252
11. Li K (2007) Ceramic membranes for separation and reaction. John Wiley & Sons Ltd, Chichester, UK
12. Jonoobi M, Mathew AP, Oksman K (2012) Ind Crop Prod 40:232
13. Wan Ngah WS, Hanafiah MAKM (2008) Bioresour Technol 99:3935
14. O'Connell DW, Birkinshaw C, O'Dwyer TF (2008) Bioresour Technol 99:6709
15. Klemm D, Kramer F, Moritz S, Lindstroem T, Ankerfors M, Gray D, Dorris A (2011) Angew Chem Int Ed 50:5438
16. Hokkanen S, Bhatnagar A, Sillanpää M (2016) Water Res 91:156
17. Liu P, Sehaqui H, Tingaut P, Wichser A, Oksman K, Mathew A (2014) Cellulose 21:449
18. Voisin H, Bergström L, Liu P, Mathew PA (2017) Nanomaterials 7:57
19. Mohammed N, Grishkewich N, Tam KC (2018) Environ Sci Nano 5:623
20. Najib N, Christodoulatos C (2019) J Hazard Mater 367:256
21. Sehaqui H, Mautner A, de Perez LU, Pfenninger N, Tingaut P, Zimmermann T (2016) Carbohydr Polym 135:334
22. Wang D (2019) Cellulose 26:687
23. Habibi Y (2014) Chem Soc Rev 43:1519
24. Rol F, Belgacem MN, Gandini A, Bras J (2019) Prog Polym Sci 88:241
25. Mautner A, Kobkeatthawin T, Mayer F, Plessl C, Gorgieva S, Kokol V, Bismarck A (2019) Nanomaterials 9:136
26. Mautner A, Kwaw Y, Weiland K, Mvubu M, Botha A, John MJ, Mtibe A, Siqeira G, Bismarck A (2019) Ind Crop Prod 133:325
27. Goi Y, Fujisawa S, Saito T, Yamane K, Kuroda K, Isogai A (2019) Langmuir 35:10920
28. Mautner A, Bismarck A (2021) Carbohydr Polym 251:117130
29. Mautner A, Lee K-Y, Lahtinen P, Hakalahti M, Tammelin T, Li K, Bismarck A (2014) Chem Commun 50:5778
30. Mautner A, Lee K-Y, Tammelin T, Mathew AP, Nedoma AJ, Li K, Bismarck A (2015) React Funct Polym 86:209
31. Karim Z, Claudpierre S, Grahn M, Oksman K, Mathew AP (2016) J Membr Sci 514:418
32. Mautner A, Maples HA, Kobkeatthawin T, Kokol V, Karim Z, Li K, Bismarck A (2016) Int J Environ Sci Technol 13:1861
33. Mautner A, Maples HA, Sehaqui H, Zimmermann T, de Perez LU, Mathew AP, Lai CY, Li K, Bismarck A (2016) Environ Sci 2:117

34. Janesch J, Jones M, Bacher M, Kontturi E, Bismarck A, Mautner A (2020) React Funct Polym 146:104428

35. Yousefi N, Jones M, Bismarck A, Mautner A (2021) Carbohydr Polym 253:117273

36. Liu P, Oksman K, Mathew AP (2016) J Colloid Interf Sci 464:175

37. Liu P, Borrell PF, Božič M, Kokol V, Oksman K, Mathew AP (2015) J Hazard Mater 294:177

38. Karim Z, Hakalahti M, Tammelin T, Mathew AP (2017) RSC Adv 7:5232